



**HAL**  
open science

# Tip-Leakage Flow: a Detailed Simulation with a Zonal Approach

Jérôme Boudet, Bo Li, Joëlle Caro, Emmanuel Jondeau, Marc C. Jacob

► **To cite this version:**

Jérôme Boudet, Bo Li, Joëlle Caro, Emmanuel Jondeau, Marc C. Jacob. Tip-Leakage Flow: a Detailed Simulation with a Zonal Approach. 22nd AIAA/CEAS Aeroacoustics Conference, May 2016, Lyon, France. pp.1-11. hal-02177963

**HAL Id: hal-02177963**

**<https://hal.science/hal-02177963>**

Submitted on 9 Jul 2019

**HAL** is a multi-disciplinary open access archive for the deposit and dissemination of scientific research documents, whether they are published or not. The documents may come from teaching and research institutions in France or abroad, or from public or private research centers.

L'archive ouverte pluridisciplinaire **HAL**, est destinée au dépôt et à la diffusion de documents scientifiques de niveau recherche, publiés ou non, émanant des établissements d'enseignement et de recherche français ou étrangers, des laboratoires publics ou privés.



## Open Archive Toulouse Archive Ouverte (OATAO)

OATAO is an open access repository that collects the work of some Toulouse researchers and makes it freely available over the web where possible.

This is an author's version published in: <https://oatao.univ-toulouse.fr/24060>

**Official URL** : <https://doi.org/10.2514/6.2016-2824>

### To cite this version :

Boudet, Jérôme and Li, Bo and Caro, Joëlle and Jondeau, Emmanuel and Jacob, Marc C. Tip-Leakage Flow: a Detailed Simulation with a Zonal Approach. (2016) In: 22nd AIAA/CEAS Aeroacoustics Conference, 30 May 2016 - 1 June 2016 (Lyon, France)

Any correspondence concerning this service should be sent to the repository administrator:

[tech-oatao@listes-diff.inp-toulouse.fr](mailto:tech-oatao@listes-diff.inp-toulouse.fr)

# Tip-Leakage Flow: a Detailed Simulation with a Zonal Approach

Jérôme Boudet <sup>\*</sup>, Bo Li <sup>†</sup>, Joëlle Caro <sup>‡</sup> and Emmanuel Jondeau <sup>‡</sup>

*Univ Lyon, Ecole Centrale de Lyon, CNRS, LMFA, F-69134, Ecully, France*

Marc C. Jacob <sup>§</sup>

*Univ Lyon, Université Claude Bernard Lyon 1, CNRS, LMFA, F-69134, Ecully, France*

*also at ISAE-SupAéro, DAEP, F-31000, Toulouse, France*

The secondary flow generated by the clearance between an isolated airfoil tip and an end-plate is analyzed by means of a zonal large-eddy simulation, in comparison with available experimental data. The flow around the tip clearance is described with full large-eddy simulation, while Reynolds-averaged Navier-Stokes is employed in the rest of the computational domain in order to limit computational cost. The various analyses of the flow characteristics (mean velocities, Reynolds stresses, spectra) show a very good agreement between the experiment and the simulation. Looking at the mean velocities, an intense tip-leakage vortex is observed on the suction side. The Reynolds stresses are used to evaluate the anisotropy of the vortex. Finally, the spectral content is investigated in the near-field and the far-field, and the leakage flow is shown to be characterized by a dominant contribution in the range  $[0.7\text{ kHz}; 7\text{ kHz}]$ .

## Nomenclature

$c$	chord length
FWH	Ffowcs-Williams and Hawkings acoustic analogy
$h$	clearance height
LES	large-eddy simulation
PIV	particle image velocimetry
RANS	Reynolds-averaged Navier-Stokes
TLV	tip-leakage vortex
$U, V, W$	Mean velocity components ( $x, y$ and $z$ components respectively)
$u', v', w'$	RMS fluctuating velocity components ( $x, y$ and $z$ components respectively)
$u'u', u'v' \dots$	Reynolds stresses
ZLES	zonal large-eddy simulation
<i>Subscript</i>	
0	Inflow conditions

## I. Introduction

In turbomachines, clearances are necessary between vanes or blades and end-walls (hub or casing) in order to allow relative movements. Such gaps result in a strong leakage flow, driven by the pressure difference and affected by the relative wall movements. When it enters the blade passage, this leakage flow produces a

---

<sup>\*</sup>Associate professor, e-mail: jerome.boudet@ec-lyon.fr.

<sup>†</sup>PhD student.

<sup>‡</sup>Engineer.

<sup>§</sup>Professor, AIAA Member.

streamwise vortex, referred to as tip-leakage vortex (TLV) and possibly other vortices (e.g. counter-rotating vortices).<sup>1</sup> At high Reynolds number, turbulence is transported and produced in this vortical flow, near the blade, and broadband noise is generated. This noise mechanism has been investigated experimentally by Kameier and Neise<sup>2</sup> for example.

Detailed experimental characterizations of the tip-leakage flow in a blade cascade have been carried out by Muthanna and Devenport<sup>3</sup> and Wang and Devenport,<sup>4</sup> with stationary and moving end-wall. This extensive work has been used as reference for a large-eddy simulation (LES) performed by You *et al.*<sup>5,6</sup> LES uses a direct description of the largest and most energetic turbulent eddies, which permits a detailed analysis of the turbulent dynamics. More recently, Pogorelov *et al.*<sup>7</sup> presented LES simulations of a five-blade rotor, with a particular attention paid to the tip-leakage flow.

In the present work, a rather simple configuration is considered: a single airfoil, between two end-plates, with a clearance at the lower end. This simplicity enabled Jacob *et al.*<sup>8</sup> to carry out a detailed experimental characterization, on both aerodynamics and acoustics. In the present paper, a zonal large-eddy simulation is introduced and compared with available experimental data.

The experimental configuration and the numerical set-up are presented in section II. The results are analyzed in section III, and the conclusions are drawn in section IV.

## II. Configuration and numerical parameters

### II.A. Experimental configuration

The experimental configuration is constituted of a single airfoil set in the potential core of a jet, between two end-plates. A sketch is shown in Fig.1. A clearance is located at the lower end of the airfoil. The chord length is  $c = 0.2$  m, the upstream velocity is  $U_0 = 70$  m/s, which yields a Reynolds number  $Re_c = 9.3 \times 10^5$  and a Mach number  $M = 0.2$ . In the original experiment, presented by Jacob *et al.*,<sup>9</sup> the angle of attack was 15 deg ( $\pm 0.5$  deg). But the experimental results used in the present paper have been obtained during a more recent campaign, presented in a companion paper from Jacob *et al.*<sup>8</sup> During this latter campaign, the angle of attack had to be set to 16.5 deg ( $\pm 0.5$  deg) in order to recover the same airfoil loading as the original experiment. The details of the experimental configuration and an analysis of the experimental results are presented in the companion paper.<sup>8</sup>

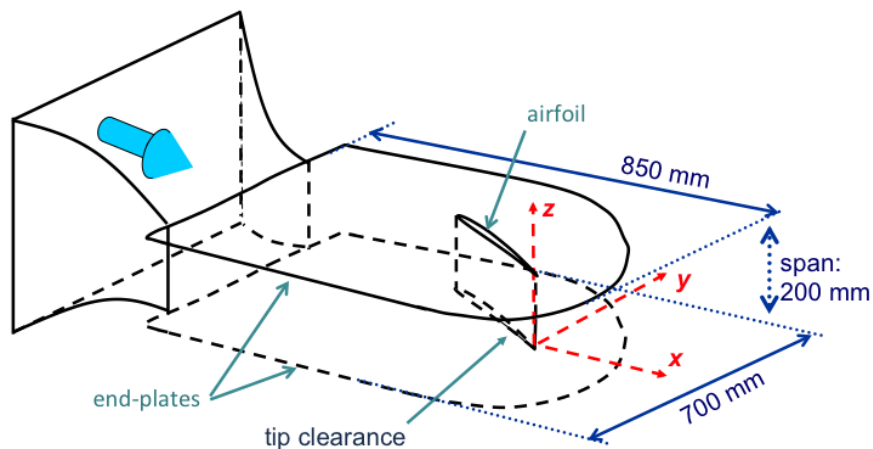


Figure 1. Experimental configuration. The origin of the coordinate system is on the blade tip / trailing edge corner, and  $z \leq 0$  in the clearance.

### II.B. Zonal Large-Eddy Simulation

The simulation uses a zonal approach. It allows to define a region of interest (in this case: around the clearance), where large-eddy simulation is used for a direct description of the most energetic turbulent eddies. In the other regions, an averaged approach (RANS) is used in order to reduce the computational cost. The formulation of the zonal approach is explained in details by Boudet *et al.*<sup>10</sup> LES relies on the shear-improved Smagorinsky model from L ev eque *et al.*,<sup>11</sup> and RANS on Wilcox's  $k - \omega$  model.<sup>12</sup> An instantaneous view of

the simulated flow field is shown in Fig.2. The turbulent eddies in the incoming boundary layer are shown to interact with the airfoil leakage flow. The TLV vortex also appears on the figure and is characterized by higher velocities.

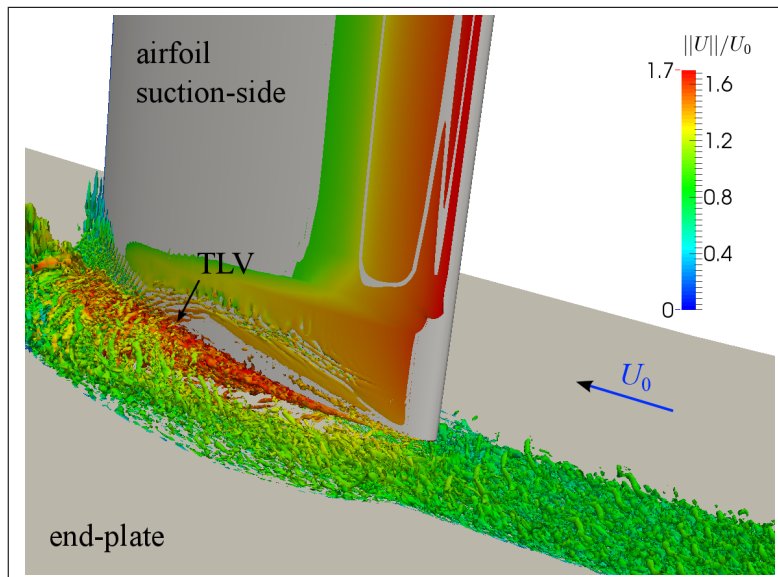


Figure 2. 3D instantaneous view of the ZLES simulation. Iso-surface of  $Q$ -criterion, colored by the velocity magnitude.

In Fig.3, instantaneous contours of velocity are shown together with the zonal decomposition of the computational domain. The region of higher velocities corresponds to the jet. It is deviated by the airfoil, and this deviation has to be taken into account to reproduce the airfoil loading, as discussed by Moreau *et al.*<sup>13</sup> Around the airfoil clearance, the LES zone corresponds approximately to the interior of the jet. Along the span, it extends up to  $5h$  above the lower end-plate. It has been positioned from a preliminary RANS computation. Most of the jet shear layers and the outer region at rest are simulated with RANS in order to alleviate the computational cost. Moreover, turbulent quantities need to be imposed at the inflow of the LES zone: the incoming boundary layer is simulated with LES over a limited width, and duplicated laterally to feed the LES.

The solver is *Turb'Flow*, an in-house finite volume code for multi-block structured grids. The inviscid flux interpolation uses a four-point centered scheme, with a fourth-order artificial viscosity in the LES zone (coefficient  $\leq 0.03$ , cf. Boudet *et al.*<sup>14</sup>) and smoothly increased artificial viscosity in the peripheral regions. The viscous flux interpolation uses a two-point centered scheme. Time marching is explicit, with a three-step Runge-Kutta scheme, and a time step of  $5.6 \times 10^{-6} c/U_0$ . Because the simulation has been initiated before the second test-campaign, the original angle of attack (15 deg) has been chosen. After convergence, results are stored every 3000 iterations over more than  $10 \cdot c/U_0$ , and flow statistics are computed on the fly.

In the LES zone, the grid resolution is:  $\Delta x^+ < 80$  (streamwise),  $\Delta y^+ < 1.5$  (wall normal) and  $\Delta z^+ < 30$  (cross-stream), for a full LES resolution of the boundary layers. The computational domain extends over  $29c$  axially,  $37c$  laterally and  $1c$  spanwise, with the end-plates extending over the whole domain. The total number of grid points is about  $150 \times 10^6$ , distributed over 524 structured blocks for parallel computing.

From the ZLES near-field results, the acoustics is computed with the Ffowcs-Williams and Hawkings<sup>15</sup> (FWH) acoustic analogy. It is implemented in the in-house solver *Turb'AcAn*,<sup>16</sup> developed from the formulation of Casalino.<sup>17</sup> Integration is performed on the airfoil surface, from the recorded flow fields, and propagation is supposed in a free-field medium (no end-plate) at rest.

A preliminary analysis of this simulation, based on a shorter sample (duration:  $6 \cdot c/U_0$ ), has been presented by Boudet *et al.*<sup>18</sup> The present paper relies on a longer sample (duration:  $10 \cdot c/U_0$ ) and introduces new analyses.

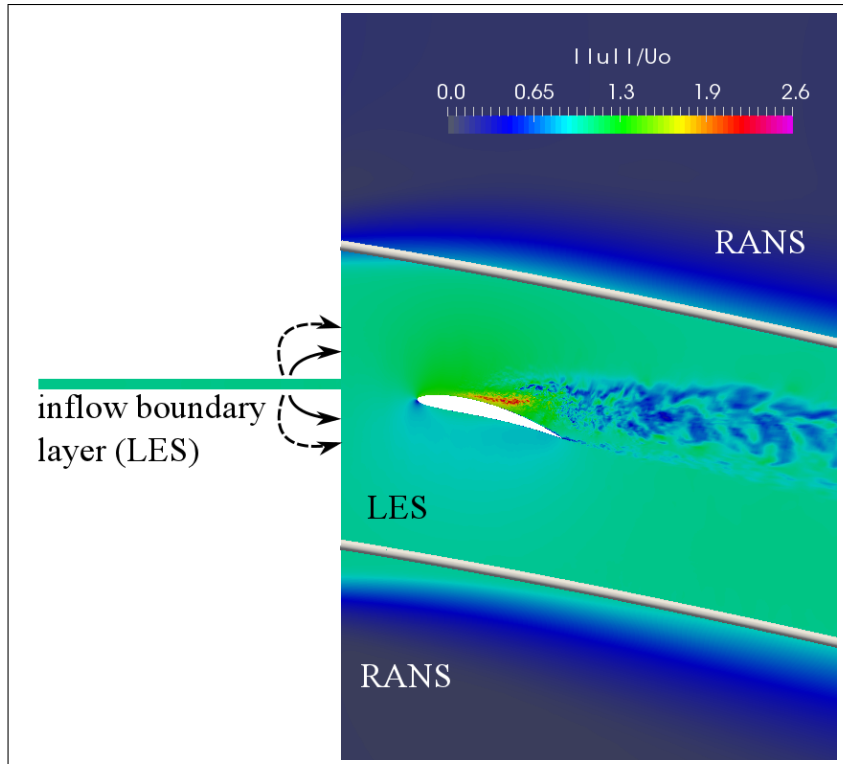


Figure 3. Instantaneous contours of the velocity magnitude around the airfoil at  $z = 0.5h$ , with indication of the LES and RANS zones (the separation between the zones is marked in light grey).

### III. Results

The present analysis essentially relies on two cross-stream planes (constant  $x$ ), located at 80% and 90% of the chord, on the suction side.

#### III.A. Mean velocity

The mean velocity distribution is plotted in Fig.4 ( $V$  component) and Fig.5 ( $W$  component). In these figures, the experimental data (PIV) are plotted on the left hand side, and the ZLES data on the right hand side. The results at 80% $c$  are on the upper line, and those at 90% $c$  on the lower line. The mean velocity vectors in the planes are also plotted to visualize the TLV.

Overall, a very good agreement is observed between the experiment and the ZLES. Some small rounded-shape regions are visible in the PIV results near the blade suction side ( $y \approx 30$  mm). These are measurement errors, due to laser reflections. The clearance below the airfoil results in a powerful jet flow, with  $V$  approaching  $1.2 \cdot U_0$  in the region  $y \lesssim 50$  mm and  $z \leq 0$ . In the continuity of this leakage flow, the TLV is identified by: positive  $V$  below, negative  $V$  above, negative  $W$  on the left hand side and positive  $W$  on the right hand side. The size and the intensity of these regions (thus of the TLV) are well reproduced by ZLES, at both axial positions. The TLV is particularly strong, with rotational velocities up to nearly  $1.2 \cdot U_0$ .

Comparing the two axial sections, the position of the TLV center is very similar, which indicates a streamwise evolution along the jet axis (given the orientation axes shown in Fig.1), and a progressive drift away from the airfoil suction side. This is consistent between the experiment and the computation, even though the TLV center appears slightly further from the walls in the ZLES.

#### III.B. Reynolds stresses

The Reynolds stresses are extracted on the plane at 90% $c$ . The six components are presented for the ZLES, but only the components  $v'v'$ ,  $w'w'$  and  $v'w'$  are available from the two-component PIV. The normal stresses are plotted in Fig.6 and the shear stresses in Fig.7. As previously noticed on the mean velocity components, measurement errors are again visible on the left hand side of the PIV figures. Apart from this specific region,

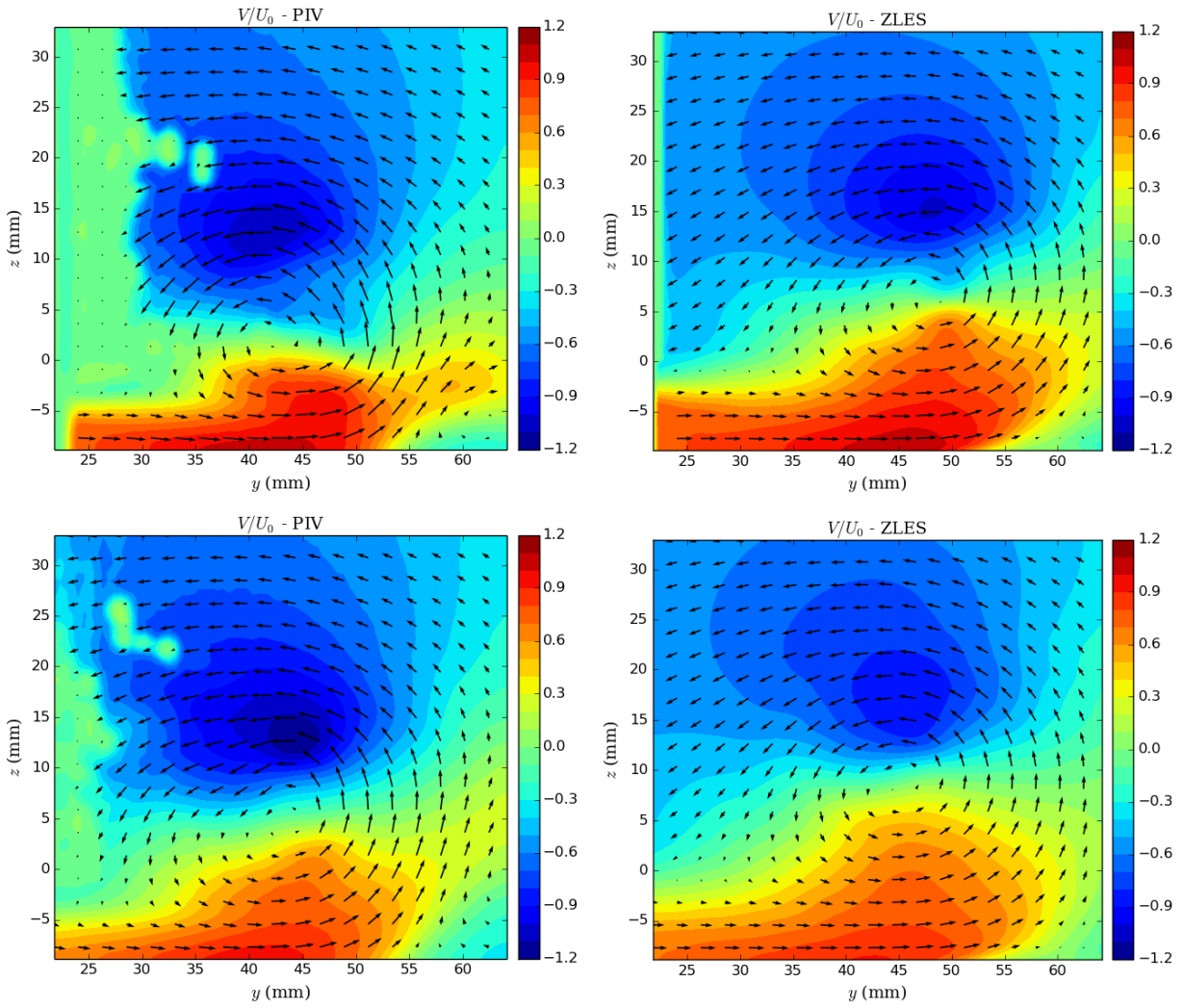


Figure 4. Mean transverse velocity  $V/U_0$ . Up: 80%c, Down: 90%c. Left: PIV, Right: ZLES.

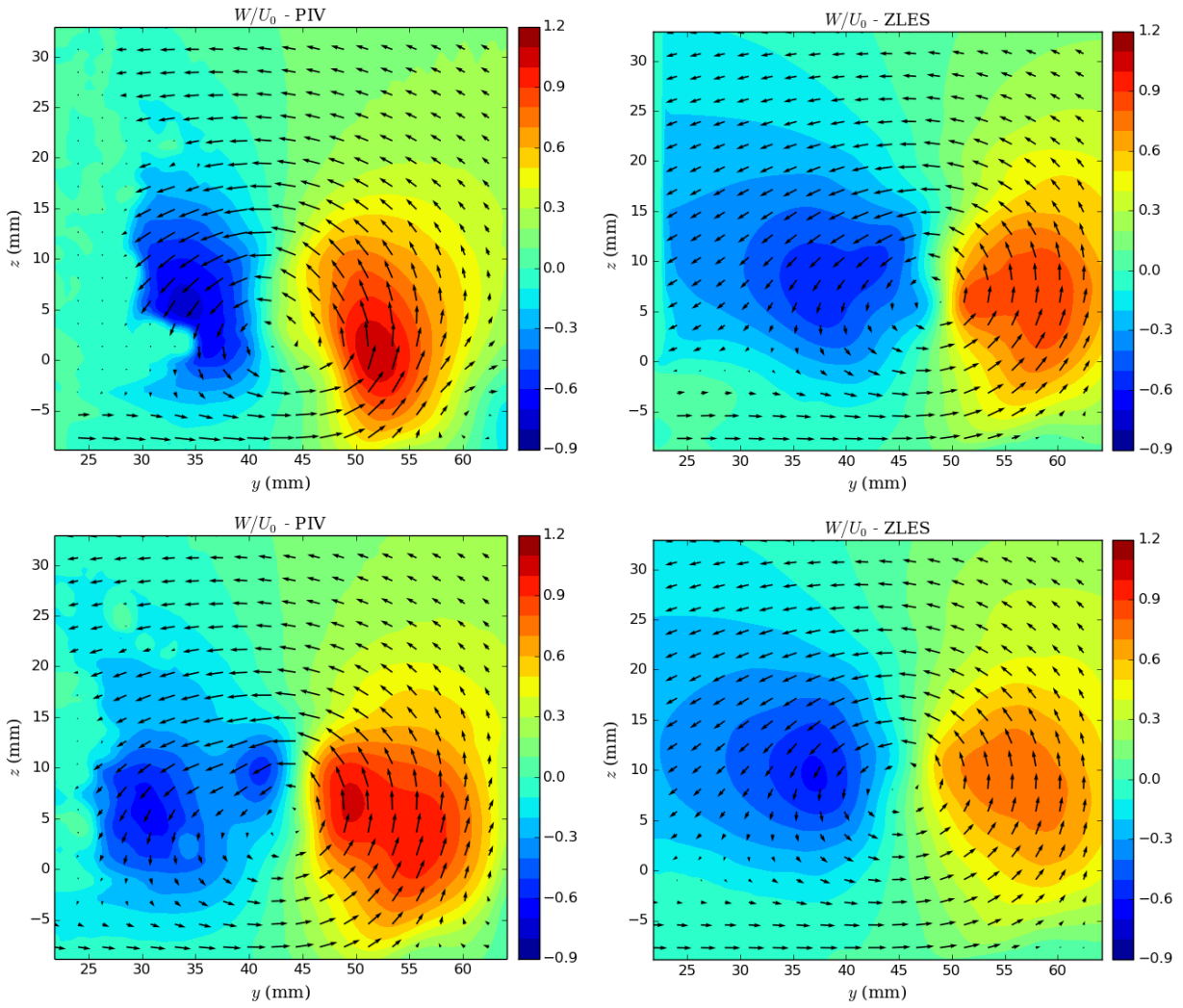


Figure 5. Mean spanwise velocity  $W/U_0$ . Up: 80%c, Down: 90%c. Left: PIV, Right: ZLES.

a good overall agreement is observed between the experiment and the ZLES. Reynolds stresses are second order statistics and are selective indicators of the simulation quality.

The normal stresses are analyzed first. Comparable levels are observed for the three components, but the stresses are distributed quite differently. For the three components, the center of the vortex is a region of intense fluctuations. A particularly high level is reached for  $w'w'$  in the PIV, but not in the ZLES. The wandering of the vortex, observed experimentally by Jacob *et al.*,<sup>8</sup> should contribute to these fluctuations. Another region of intense normal stresses is observed, for the three components, in the continuity of the clearance ( $y \leq 45$  mm and  $z \approx -5$  mm). The powerful jet flow through the clearance, observed in Fig.4, is associated with intense turbulence. One region of intense normal Reynolds stresses appear essentially on one component ( $v'v'$ ), for  $y \approx 55$  mm and  $z \lesssim 0$ . This region of anisotropy is associated with the drag of the TLV on the end-plate boundary-layer. It appears in both the experiment and the computation, but is more intense in the latter. Finally, in the ZLES, one can observe the regions of higher normal Reynolds stresses are distributed differently on the right hand side of the TLV for the three components. This is another deviation from turbulence isotropy within the TLV.

The Reynolds shear stresses are presented in Fig.7. They gauge the level of anisotropy of the flow, since they are null for isotropic turbulence. The values appear significant, compared with the normal stresses, particularly for  $v'w'$ . Looking at this component, the higher levels are found in the leakage flow and on the right hand side of the TLV, above the drag region of the TLV on the end-plate boundary layer. The agreement between the experiment and the simulation is good again, except some over-estimate of the intensity by ZLES on the right hand side of the TLV. The other two components ( $u'v'$  and  $u'w'$ ) are only available from ZLES. Though less intense than  $v'w'$ , these two components show notable spatial evolutions through the TLV.

### III.C. Near-field and far-field spectra

The strength of LES lies essentially in the description of a major part of the turbulent spectrum, from the point of view of turbulent kinetic energy. For the present configuration, Fig.8 presents wall pressure spectra on the suction and pressure sides, at 77.5% $c$  and just 1.5 mm above the blade tip. A good agreement is observed between the experiment and the simulation. The ZLES over-estimates the levels on the suction side (probe 21) by about 5dB, and the spectrum shape is fairly well predicted. On the pressure side, where turbulence intensity is lower, a remarkable agreement is achieved between the experiment and the simulation. This concerns both the levels and the singular shape of the spectrum. Indeed, the spectrum is characterized by a hump around  $f = 1292$  Hz. This must be associated with the tip-clearance flow, and is also visible on the suction side, but stands out less clearly probably because broadband turbulence is more intense. This frequency, when normalized with the inflow velocity  $U_0$  and the gap height  $h$  as a Strouhal number, gives  $St = f.h/U_0 = 0.18$ . From a physical point of view about vortical flows, one can notice this Strouhal value is consistent with those measured for the vortex shedding behind a circular cylinder, for example.

Finally, the acoustic spectrum at 2 m aside the airfoil, on the suction side, is plotted in Fig.9. The computed spectrum (FWH propagation from the ZLES results) is compared with the experimental spectrum. A very good agreement is observed in the central frequency range [0.7 kHz; 7 kHz]. At lower frequencies, the experimental spectrum is probably affected by installation noise, i.e. various noise sources associated with the experimental rig around the tip-flow configuration. At higher frequencies, the under-prediction of the simulation may be explained by the RANS description of most of the blade-span (15 cm out of 19 cm). Indeed, RANS does not predict the airfoil self-noise sources at the trailing-edge, which are expected to contribute to the high-frequency content of the spectrum because of the relatively small length scales involved (boundary layer...). The central frequency range, where a very good match is observed, corresponds to the tip-leakage contribution previously identified by a hump in the near-field spectra. Logically, the confinement of the LES resolution around the clearance makes the related noise sources stand out in the acoustic spectrum. This range of influence of the leakage flow has been also identified in the experiment, by comparison with a no-leakage set-up, and the present observation can be seen as a confirmation through a numerical approach.

## IV. Conclusion

A zonal simulation of an academic tip-leakage flow has been presented, and compared with detailed flow and acoustic measurements. The configuration is made of a single airfoil set above a flat plate, with a

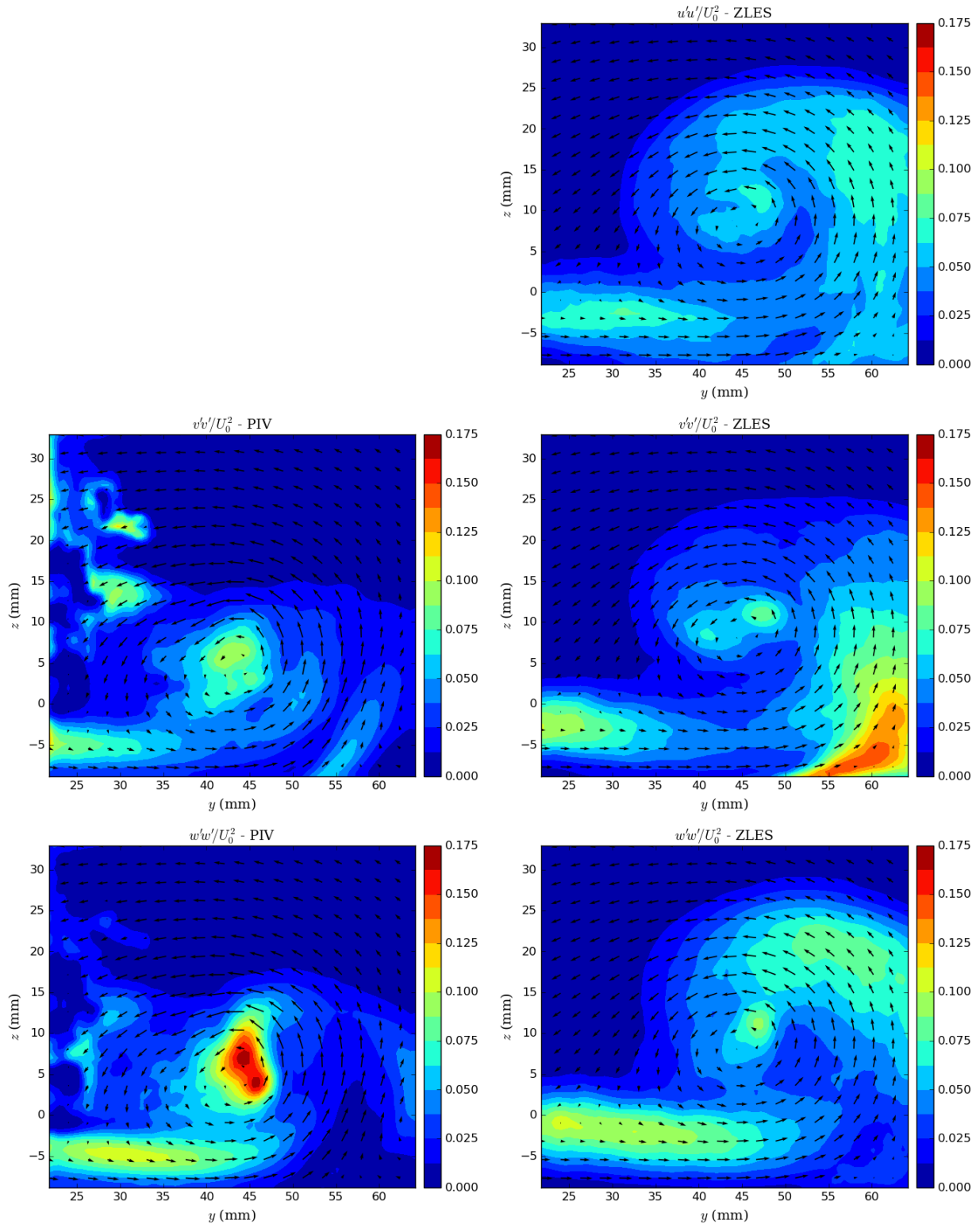


Figure 6. Normal Reynolds stresses at 90%c. Left: PIV, Right: ZLES.

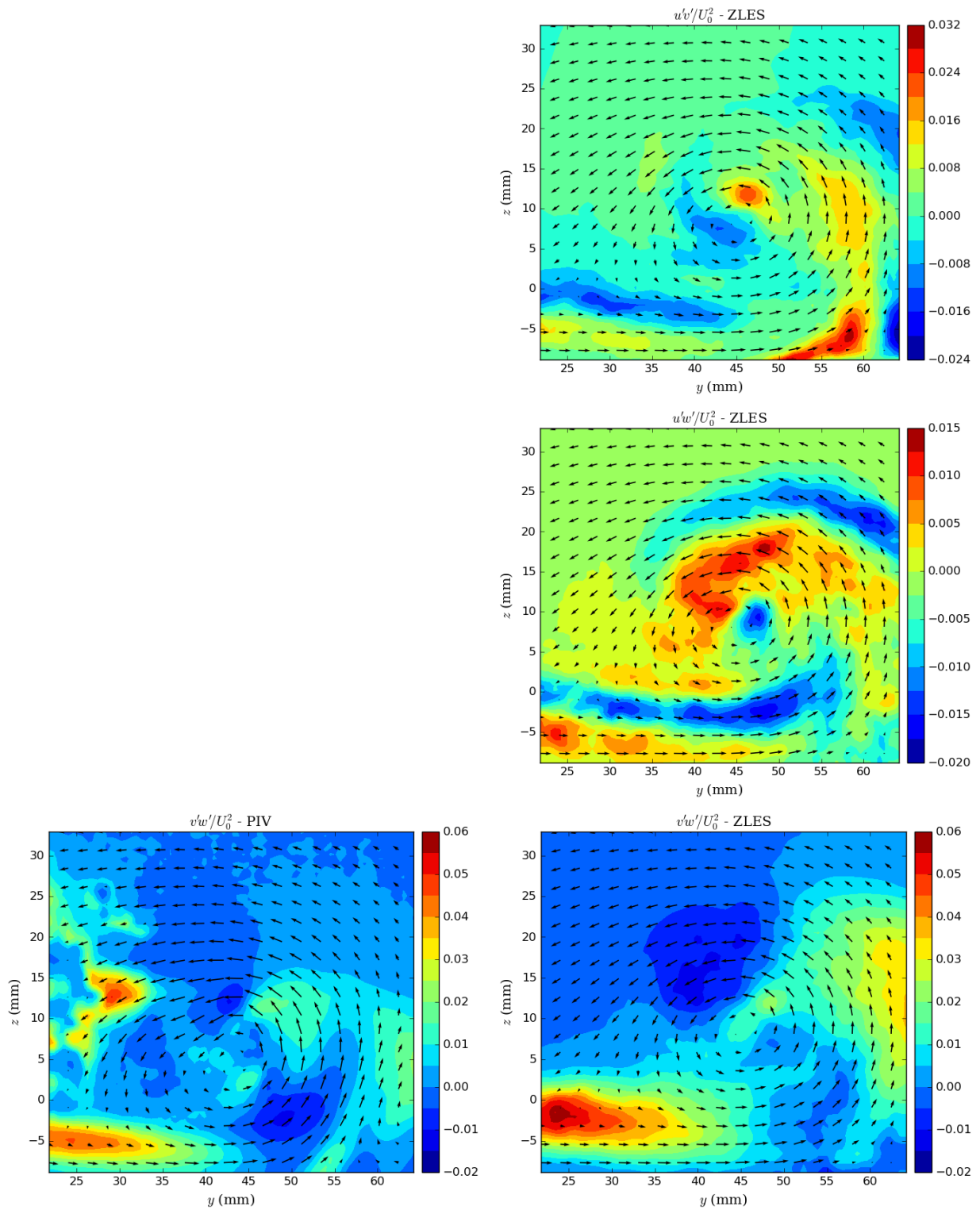


Figure 7. Reynolds shear stresses at 90%c. Left: PIV, Right: ZLES.

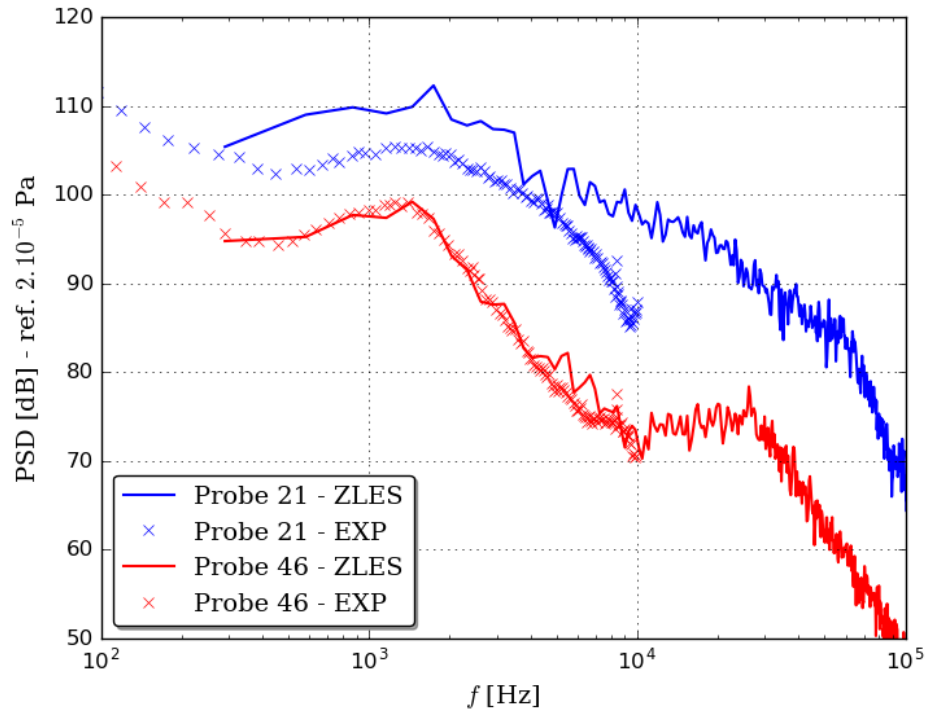


Figure 8. Pressure spectra on the airfoil suction side (probe 21) and pressure side (probe 46), at 77.5%*c* and just 1.5 mm above the blade tip.

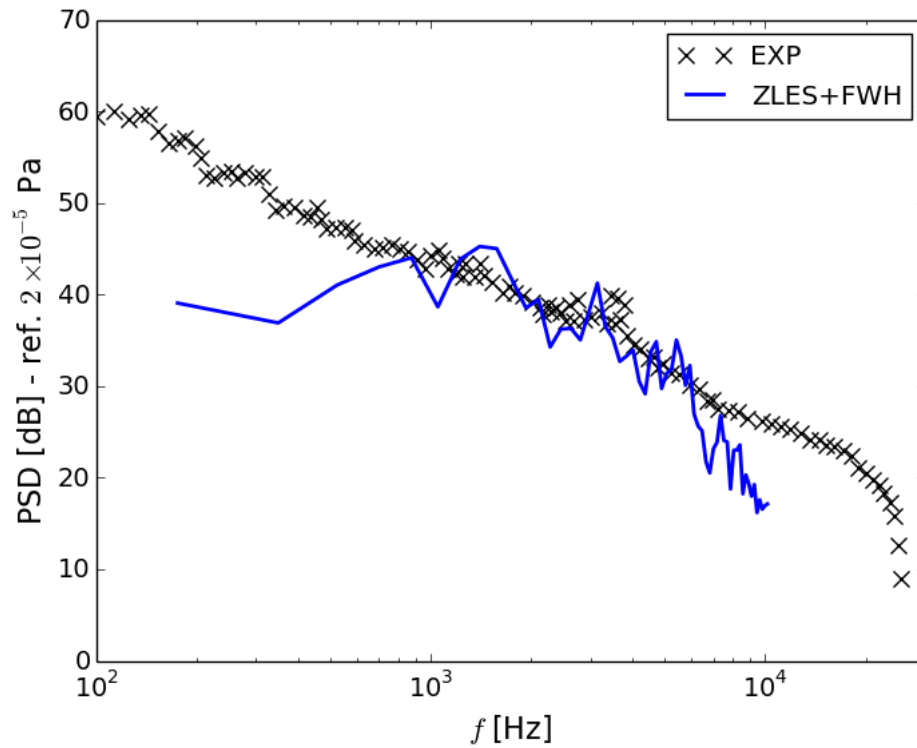


Figure 9. Far field acoustics, at 2 m from the airfoil, along *y*-direction. For the simulated spectrum (ZLES+FWH), the time sample is split into 9 blocks, with 50% overlap, and the corresponding spectra are averaged for smoothing.

clearance in-between. The advanced LES approach is confined to the region of interest around the airfoil clearance, and classical RANS is used elsewhere in order to limit computational cost.

The simulation provides a good description of the mean transverse velocities, on cross-stream planes at 80% $c$  and 90% $c$ . The TLV is particularly intense, with rotational velocities approaching  $1.2 \cdot U_0$ . The size and intensity of the TLV are well reproduced by the ZLES.

The simulation also gives a good description of the Reynolds stresses. Intense fluctuations are found in the leakage flow, at the TLV center, and around the drag region in the end-plate boundary layer. The flow in the TLV is anisotropic, as shown by the significant Reynolds shear stress values.

A good simulation of the spectral content is also achieved. This has been shown in the near-field of the clearance, where the spectra are characterized by a hump around the Strouhal number  $St = 0.18$ . A good description is also achieved in the far-field, over a wide range of frequencies [ $0.7\text{ kHz}$ ;  $7\text{ kHz}$ ] attributed to the effect of the leakage flow.

This paper constitutes a validation of the simulation and shows the capabilities of a zonal approach. It also confirms the spectral range of influence of the leakage flow. The detailed results of the simulation (3D and high-frequency resolution) can now be used for an in-depth analysis of the noise mechanisms in the leakage flow.

## Acknowledgments

This work has been carried-out in the frame of the Sino-French project AXIOOM, funded by ANR and NSFC. It was granted access to the HPC resources of CINES under the allocation c20152a5039 made by GENCI (Grand Equipement National de Calcul Intensif).

## References

- <sup>1</sup>Lakshminarayana, B., *Fluid dynamics and heat transfer of Turbomachinery*, John Wiley and Sons, Inc., Hoboken, NJ, 1996.
- <sup>2</sup>Kameier, F. and Neise, W., "Experimental Study of Tip Clearance Losses and Noise in Axial Turbomachines and Their Reduction," *Journal of Turbomachinery*, Vol. 119, No. 3, July 1997, pp. 460–471.
- <sup>3</sup>Muthanna, C. and Devenport, W. J., "Wake of a Compressor Cascade with Tip Gap, Part 1: Mean Flow and Turbulence Structure," *AIAA Journal*, Vol. 42, No. 11, 2004, pp. 2320–2331.
- <sup>4</sup>Wang, Y. and Devenport, W. J., "Wake of a Compressor Cascade with Tip Gap, Part 2: Effects of Endwall Motion," *AIAA Journal*, Vol. 42, No. 11, 2004, pp. 2332–2340.
- <sup>5</sup>You, D., Wang, M., Moin, P., and Mittal, R., "Vortex Dynamics and Low-Pressure Fluctuations in the Tip-Clearance Flow," *Journal of Fluids Engineering*, Vol. 129, No. 8, 2007, pp. 1002.
- <sup>6</sup>You, D., Wang, M., Moin, P., and Mittal, R., "Large-eddy simulation analysis of mechanisms for viscous losses in a turbomachinery tip-clearance flow," *Journal of Fluid Mechanics*, Vol. 586, 2007, pp. 177–204.
- <sup>7</sup>Pogorelov, A., Meinke, M., and Schröder, W., "Cut-cell method based large-eddy simulation of tip-leakage flow," *Physics of Fluids (1994-present)*, Vol. 27, No. 7, July 2015, pp. 075106.
- <sup>8</sup>Jacob, M., Jondeau, E., Li, B., and Boudet, J., "Tip Leakage Flow: Advanced Measurements and Analysis," *22nd AIAA/CEAS Aeroacoustics Conference*, Lyon, May 2016.
- <sup>9</sup>Jacob, M. C., Grilliat, J., Camussi, R., and Caputi Gennaro, G., "Aeroacoustic investigation of a single airfoil tip leakage flow," *International Journal of Aeroacoustics*, Vol. 9, No. 3, 2010, pp. 253–272.
- <sup>10</sup>Boudet, J., Cahuzac, A., Kausche, P., and Jacob, M., "Zonal large-eddy simulation of a fan tip-clearance flow, with evidence of vortex wandering," *Journal of Turbomachinery*, Vol. 137, No. 6, June 2015.
- <sup>11</sup>Lévêque, E., Toschi, F., Shao, L., and Bertoglio, J. P., "Shear-improved Smagorinsky model for large-eddy simulation of wall-bounded turbulent flows," *Journal of Fluid Mechanics*, Vol. 570, 2007, pp. 491–502.
- <sup>12</sup>Wilcox, D., "Reassessment of the scale-determining equation for advanced turbulence models," *AIAA Journal*, Vol. 26, No. 11, 1988, pp. 1299–1310.
- <sup>13</sup>Moreau, S., Henner, M., Iaccarino, G., Wang, M., and Roger, M., "Analysis of Flow Conditions in Freejet Experiments for Studying Airfoil Self-Noise," *AIAA Journal*, Vol. 41, No. 10, 2003, pp. 1895–1905.
- <sup>14</sup>Boudet, J., Monier, J.-F., and Gao, F., "Implementation of a roughness element to trip transition in large-eddy simulation," *Journal of Thermal Science*, Vol. 24, No. 1, Jan. 2015.
- <sup>15</sup>Ffowcs-Williams, J. E. and Hawkins, D. L., "Sound Generated by Turbulence and Surfaces in Arbitrary Motion," *Philosophical Transactions of the Royal Society*, Vol. A264, No. 1151, 1969, pp. 321–342.
- <sup>16</sup>Boudet, J., Lévêque, E., Borgnat, P., Cahuzac, A., and Jacob, M., "A Kalman filter adapted to the estimation of mean gradients in the large-eddy simulation of unsteady turbulent flows," *Computers and Fluids*, Vol. 127, March 2016, pp. 65–77.
- <sup>17</sup>Casalino, D., "An advanced time approach for acoustic analogy predictions," *Journal of Sound and Vibration*, Vol. 261, No. 4, 2003, pp. 583–612.
- <sup>18</sup>Boudet, J., Caro, J., Li, B., Jondeau, E., and Jacob, M., "Zonal large-eddy simulation of a tip-leakage flow," *submitted to the International Journal of Aeroacoustics*, 2015.